CHAPTER-IV

CHAPTER IV

STUDIES ON PHOTOELECTROCHEMICAL (PEC) CELLS BASED ON Sb_2S_3 PHOTOELECTRODE

4.1 Introduction 67

4.2 Electrochemistry of a Semiconductor/Electrolyte Interface 68

4.2.1 Double layer at the interface 69

a] Electrolyte side of the interface

b] Semiconductor side of the interface

c] Effect of surface states and surface adsorbed ions.

4.2.2 Mechanism of charge transfer at S/E interface 83

a] Charge transfer in dark

b] Charge transfer in light

4.2.3 Some useful parameters 89

4.3 Experimental Procedure 91

4.3.1 Preparation of Sb_2S_3 photoelectrode 91

4.3.2 Electrical characterisation of a PEC cell 91

4.3.3 Optical characterisation of a PEC cell 93

a] Photoresponse

b] Spectral response

c] Speed of response

4.4 Discussion of Results 94

4.4.1 Electrical studies 95

a] Current-voltage characteristic in dark

b] Capacitance-voltage characteristic in dark

c] Power output characteristic in light

4.4.2 Optical studies 103

a] Photoresponse

b] Spectral response

c] Speed of response

4.5 Conclusions 107

4.1 Introduction

Although, semiconductor/electrolyte junctions are simple and easier to device, their properties are extremely sensitive almost to the properties of the semiconductor photoelectrode. Thus the prehistory of the photoelectrode material (by the way of preparation method, properties etc.) is need to know. The changes in properties of the photoelectrode material drastically change the photoelectrochemical behaviour of the material. Especially, the impedement of the charges across the interface, generation of a photocurrent and a photovoltage in a cell are closely related to the properties of the semiconductor electrode, an electrolyte, and the quality of the junction between them. Thus thorough understanding of the different properties of the active material is highly essential and has already formulated the development of block building of Chapter-III.

The semiconductors which possess appropriate bandgaps (1.2 to 1.7 eV) with respect to the maximum span of the solar spectrum, high coefficient of absorption, and direct mode of transition, are effective in photoelectrochemical conversion |5|. Antimony trisulphide seems to be a promising candidate in this respect since it shows a strong absorption of light of wavelength shorter than 750nm. The literature data so far reported, throw some light on the photoconducting properties of the material |24,35,36,58|, but not on the photovoltaic properties. Only a few preliminary reports |31,61,62| on the photoelectrochemistry of the Sb_2S_3 are available. Therefore, we thought it to be interesting to investigate the eletrcochemical photovoltaic

properties of the cell consisting of thin film Sb_2S_3 photoelectrode. The structural, electrical, and optical properties of Sb_2S_3 those decide its use as a photoelectrode in PEC cell are discussed in chapter III. The relevant theoretical background both in dark and in light is given in section 4.2. The necessary experimental processing steps are described inbrief in section 4.3. Section 4.4 highlights some of our experimental observations on photoelectrochemical cells formed with this material.

4.2 Electrochemistry of a Semiconductor/Electrolyte Interface

The key concept in the working of PEC Solar cells is the basic charge transfer process across the electrode/ electrolyte interface that results into the flow of current through the junction formed by a semiconductor and an electrolyte. Reports are now available those throw some light on the analogy between the semiconductor and an electrolyte as |63,64| : i] the oxidised and reduced species are analogous, respectively to the conduction and valance bands, ii] a term E_{Fredox} can also be defined similar to a semiconductor Fermilevel E_F, iii] the energy necessary to transfer an electron from the reduced species to the oxidised species is analogous to the band gap `E_g' of a semiconductor, and iv] redox potential is a potential required to transfer an electron from a redox species to a vacuum level or vice versa. The analogy between a semiconductor and an electrolyte is not perfect as the charge carriers in the two phases are different. In the semiconductors, the environment seen by an electron is an "electron cloud" and that in electrolytes the environment seen by

an ion is an "ion cloud". As the two phases are distinctly different, it would be interesting to know what happens when the two are brought in contact. At the interface, an ion is under the two forces one due to ions of an electrolyte and other due to the electrode. This anisotropy of forces at the boundary results in a new arrangement of solvent dipoles, ions of the electrolyte, and electrons of the electrode to accumulate near the surface as shown in Fig.4.1. When there is a sufficient build up of charges on both sides the electrical forces at the surface overpower the barrier resulting in the flow of charges.

An equilibrium is established, of the type -

$$E_s = E_l \qquad \ldots (4.1)$$

where E_s and E_l are electrochemical potentials on the semiconductor and electrolyte sides, respectively. Thus the potential gradient associated with the interface, which is high at the surface and decays gradually as we move away from it, acts as a barrier for the further flow of charges. This gives rise to a formation of double layer.

4.2.1 Double layer at the interface

Fig. 4.1 shows that the electrode/electrolyte interface which gets rectified as a result of redistribution of charges near the boundary. At the boundary interface, the charge neutrality occurs as :

$$q_s = q_{el} \qquad \ldots (4.2)$$

where q_s and q_{el} are, respectively charges near the semiconductor and electrolyte sides of the interface. To examine the structure of the double layer, we divide the interface into two regions

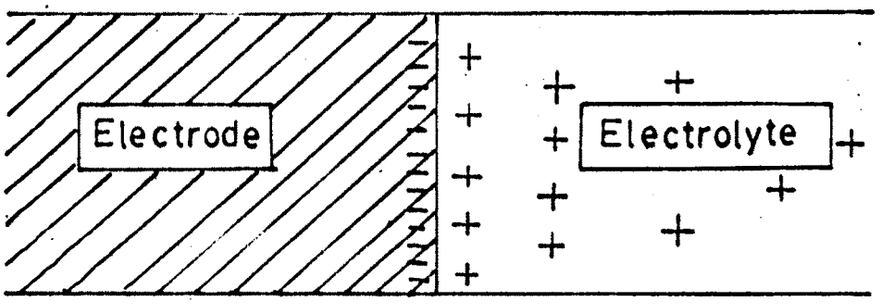

Fig.4.1 Qualitative description of charge distribution near the electrode/electrolyte interface.

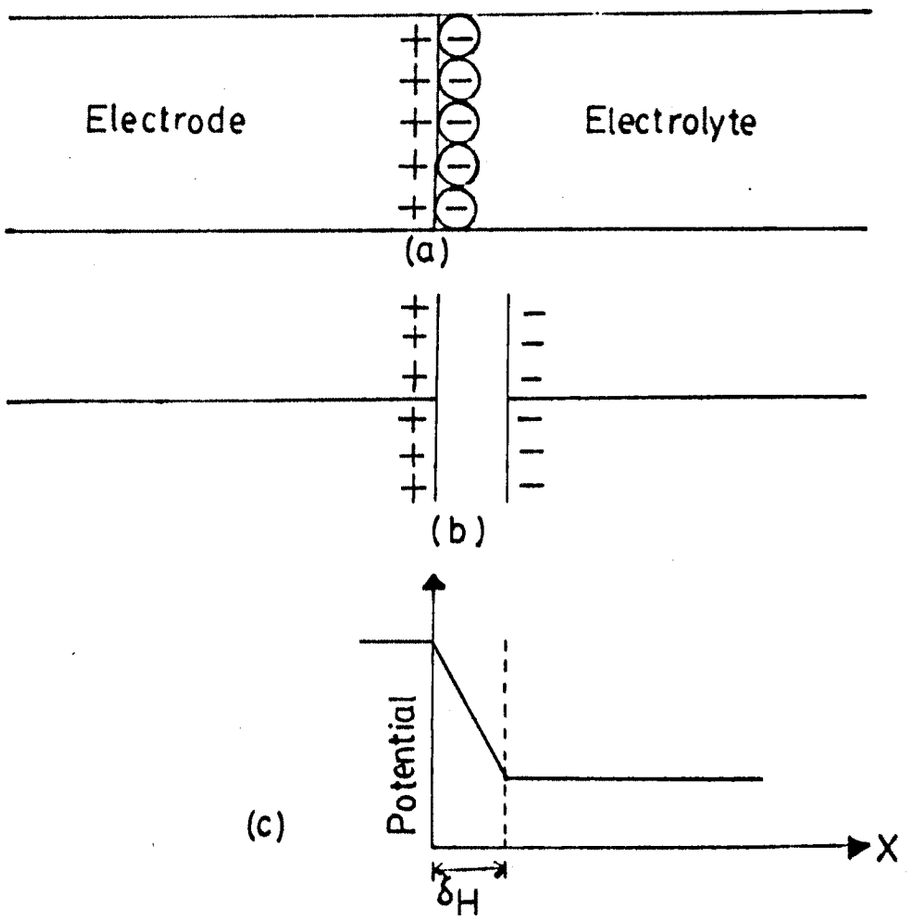

Fig.4.2 Helmholtz-Perin model :

a) Schematic charge distribution

b) Electrical equivalent of interface

c) Potential distribution towards the electrolyte.

a] electrolyte side of the interface and b] electrode side of the interface.

a] Electrolyte side of the interface

Helmholtz |65| assumed that the charged layers of ions form a sheath at the dipped metal surface as shown in Fig.4.2 (a). The Helmholtz-Perrin model suggests that the electrode/electrolyte interface is a parallel plate condenser charged oppositely with equal charges as shown in Fig.4.2 (b) and therefore, the term double layer originated. All the potential is assumed to be dropped across the thickness of a double layer (δH). If the charge on the capacitor is dQ and potential across the layer is dV, then the differential capacitor is given by :

$$C = \frac{dQ}{dV} = \frac{\epsilon\epsilon_o}{\delta H} \quad [\text{ where } \delta H = \epsilon\epsilon_o \frac{dV}{dQ}] \qquad ...(4.3)$$

where ϵ_o and ϵ are the dielectric constants of the free space and material, respectively. Initially δH was assumed to be independent of voltage V or the capacity C, which was against the experimental observations. However, Gouy |66| and chapman |67| suggested that the electrode surface, on which charges have accumulated, may be considered as a large central ion exerting a planar electrostatic field on the solution side of the interface. This force falls of slowly as one moves deeper into the solution bulk away from the electrode surface and the ions form a diffused layer called as "Gouy Layer" as shown in Fig.4.3 (a). In Fig.4.3(b,c), approximate potential and charge distribution according to G-C theory is shown. The charge distribution is given by :

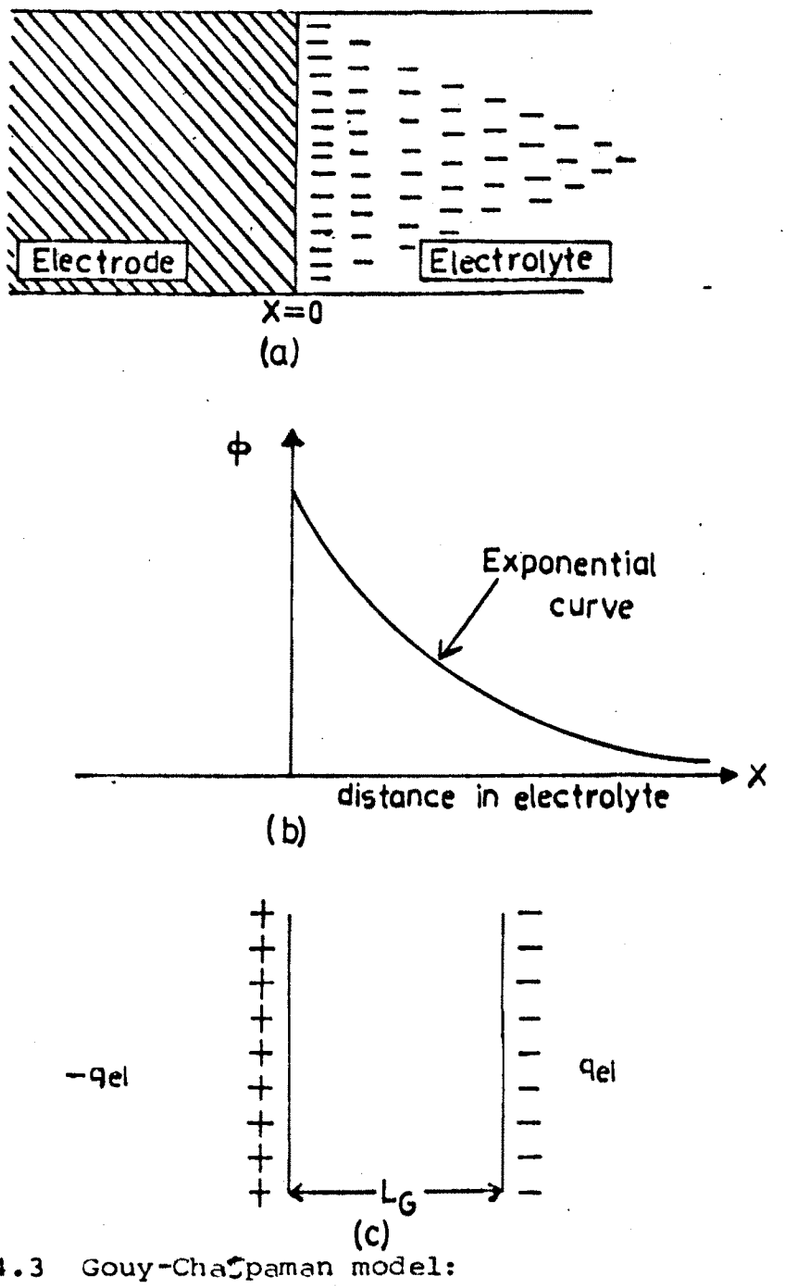

Fig-4.3 Gouy-Chapman model:

a) Schematic charge distribution

b) Potential distribution in the electrolyte

c) Simulated electrical equivalent.

BARR. BALASAHEB KHARDEKAR LIBRARY
SHIVAJI UNIVERSITY KOLHAPUR

$$\Phi_{(x)} = \Phi_{(o)} \exp(-L_G X) \qquad \ldots(4.4)$$

where, $\Phi_{(x)}$ = potential at any distance X in electrolyte, $\Phi_{(o)}$ = potential at X=0 and L_G = Gouy layer thickness or Debye length. It was found that : i] charge density distribution in Gouy Layer decays exponentially with distance in the electrolyte, ii] thickness, L_G [Fig.4.3(c)] varies inversely with square root of the ionic concentration, and iii] differential capacity of the Gouy Layer is voltage and concentration dependent. It was Stern who pointed out that the double layer is neither abrupt nor diffused but a combination of the two |68| as shown in Fig.4.4(a). Here interface distribution is divided in to two layers : i] dense ions stuck to the electrode and potential distribution is linear, ii] diffused-potential decays exponentially [Fig.4.4(b)]. The Stern model does not explain explicitly how the ions stuck to the electrode. However, it is found that the ions sit in close contact of the electrode by pushing some water molecutes away. The ions so sitting are called "contact adsorbed ions". The locus of all such contact adsorbed ions form the "Inner Helmholtz Plane (IHP)". The solvated ions are in the "Outer Helmholtz Plane (OHP). The situation is shown in Fig.4.4(c).

Thus a picture of electrolyte side of the interface can be summarised as :

i] the IHP consisting of water dipoles and specifically adsorbed ions which forms a saturated dielectric layer with a dielectric constant equal to 6.

ii] the OHP consisting of solvated ions (at a distance of their

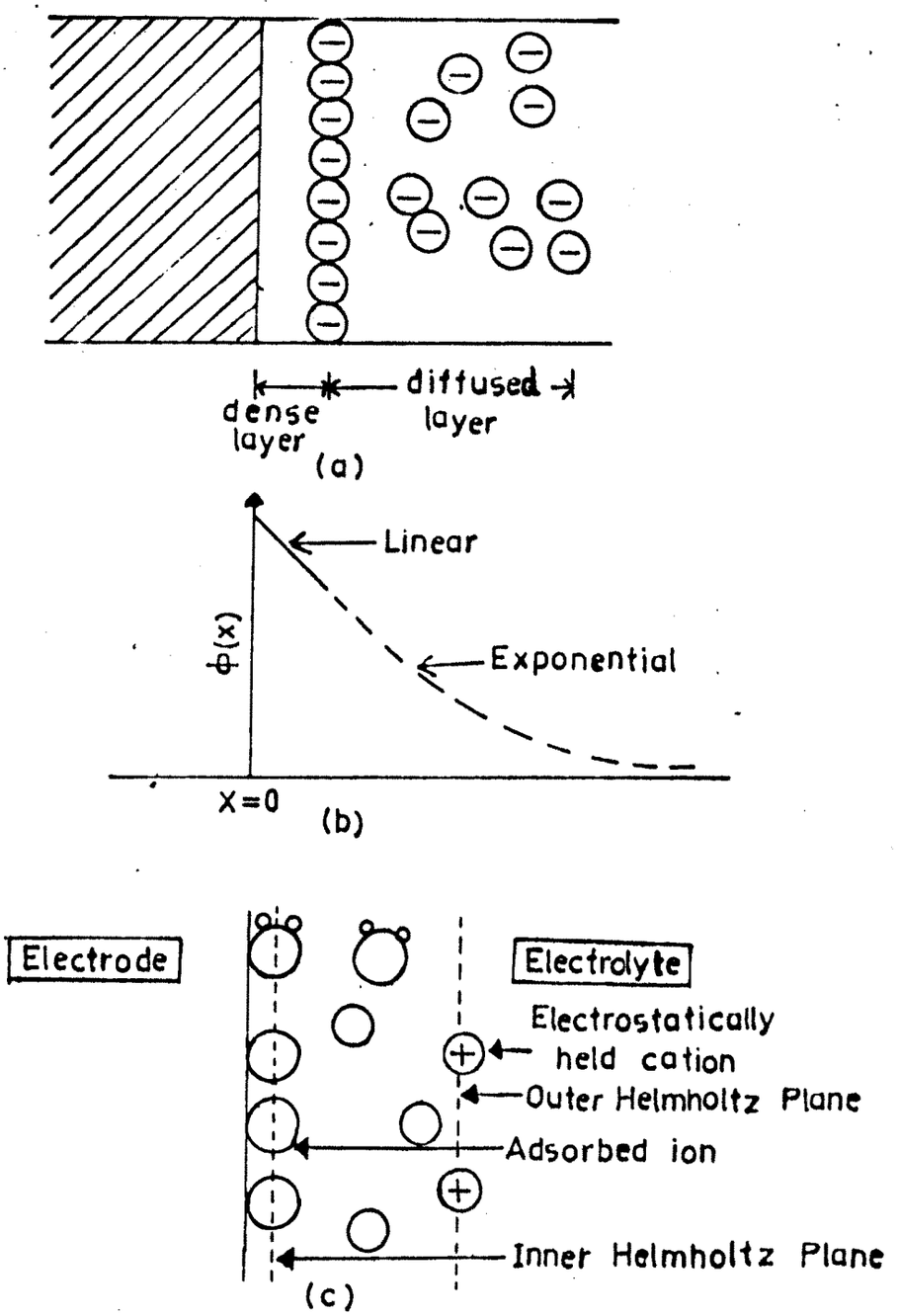

Fig-4.4 Stern model:

a) Schematic charge distribution.

b) Potential distribution

c) Relative positions of inner and outer Helmholtz planes of electrode/electrolyte interface.

closest approach to the electrode surface) with a dielectric constant between 6 and 78. A mean value of about 40 is usually taken.

iii] Gouy layer due to diffused ionic layer. For all practical purposes, G-C-S theory is correct at low ion concentration and fails for high ionic concentrations. Recently, Liu has developed a Lattice Gas model where both ions and solvent molecules are taken as hard spheres of equal radii forming a parallel layers near the planar electrode. The lattice parameter is chosen as the distance of closest approach. This model gave a reasonable description of the properties of the electrolyte in the interface region and is better than the all earlier models.

b] Semiconductor side of the interface

It may be recalled that the charge distribution of the electrode side is widely different for metals and semiconductors, principally because |63,68-70|:

i] electrons and holes are charge carriers in semiconductors while in metals only electrons carries the charges.

ii] carrier density in the semiconductors is (10^{16} to 10^{23} cm^{-3}) as against in metals (10^{28} cm^{-3}).

iii] for metals the charges are located at the surface while for semiconductors they forms a space charge layer within the semiconductor near the interface.

The potential and charge distribution on the electrode side of the semiconductor - electrolyte and metal-electrolyte interfaces are given in Fig 4.5 (a,b). The nature of the space

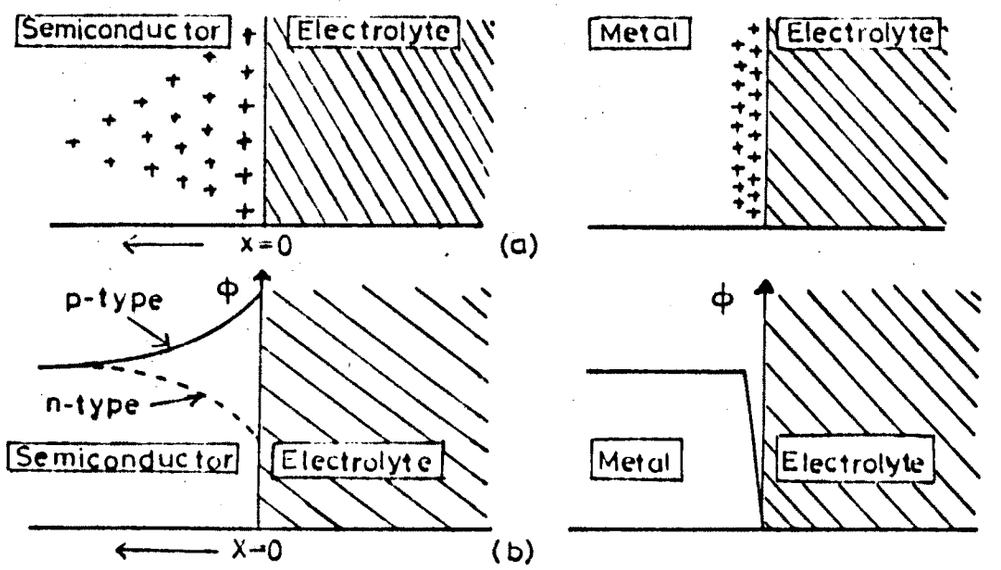

Fig.4.5 Difference between metal/electrolyte and semiconductor/electrolyte interface :
a) Charge distribution b) Potential distribution

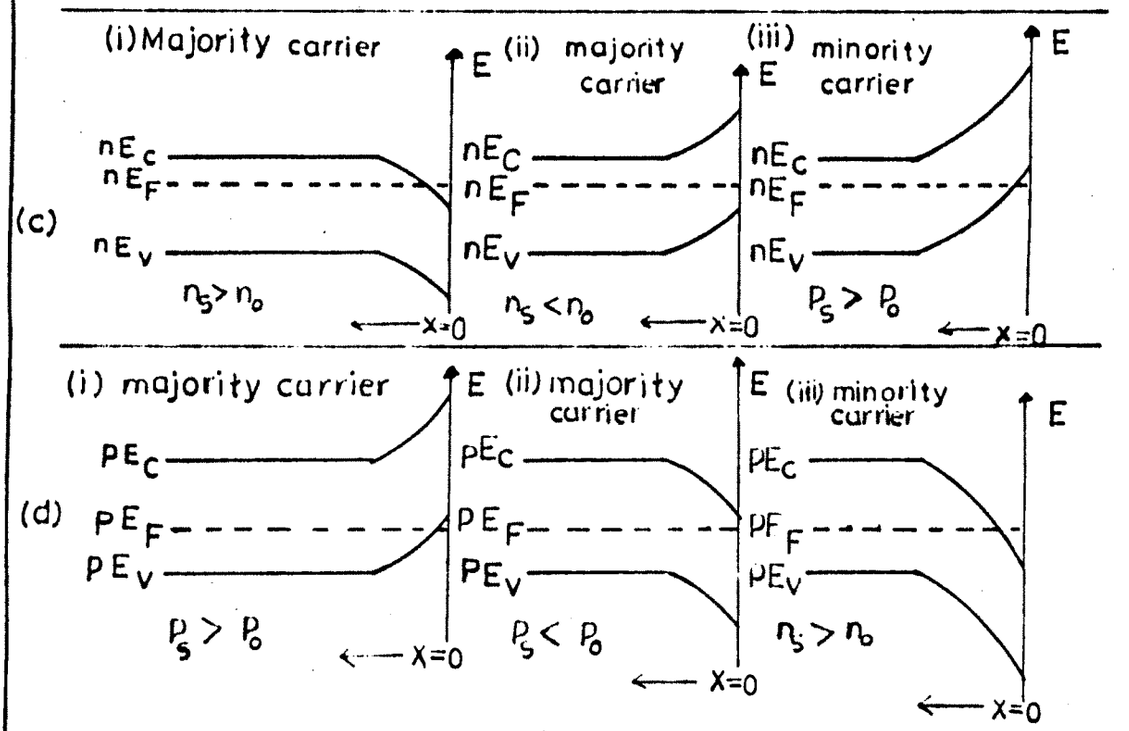

Fig. 4.5 Three types of space charge layers namely enrichment, depletion and inversion at :

c) n - type semiconductor

d) p - type semiconductor

charge layer depend up on the manner in which change transfer occurs across the interface. Three types of situations can arise.

i] if a semiconductor acquires excess majority carriers, the space charge layer is termed an "enrichment layer". Such a layer leads downward band bending for n-type while upward for p-type semiconductors.

ii] if surface becomes depleted of majority carriers then space charge is known as "depletion layer". This leads to the upward band bending for p-type semiconductors.

iii] if the charge distribution is such that the minority carrier concentration at the surface is greater than that within the bulk. Space charge layer under this condition is called as "inversion layer". This leads to a large upward band bending for n-type and downward for p-type. The above three situations are shown in Fig 4.5 (c,d).

c] Effect of surface states and surface adsorbed ions

The potential and charge distribution at the electrode-electrolyte interface are affected by the presence of surface states and surface adsorbed ions at the interface. Surface states are essentially the results of non-periodicity of the lattice at the boundary and the adsorption of foreign atoms or ions at the interface. The surface states act as the traps for charge carriers and hence substantially modify the space charge, Gouy, and Helmholtz layers and the charge and potential distribution in the various regions of the electrode-electrolyte interface.

Thus resulting picture of the semiconductor/ electrolyte interface consists of the : i] diffused space charge layer in the semiconductor (including surface states and surface adsorbed ions), ii] Helmholtz layer, iii] Gouy layer. The total charge on the semiconductor side of the interface is, $q_s = q_{sc} + q_{ss} + q_{ads}$ and the electroneutrality demands :

$$q_s = q_{sc} + q_{ss} + q_{ads} = q_{el} \qquad ...(4.5)$$

where q_{sc}, q_{ss}, q_{el}, q_{ads} corresponds respectively to charges in the space charge, surface states, electrolyte, and due to adsorbed ionic groups. The actual distribution of charge carriers may be quite complicated and it is doubtful whether M.B. or F.D. statistics are applicable to the theory of space charge layer under strong field at the boundary. The total potential (Φ_{Ga}) associated with a S/E interface is :

$$\Phi_{Ga} = \Phi_{sc} + \Phi_G + \Phi_H + \Phi_{ss} \qquad ...(4.6)$$

For concentrated electrolyte solutions, potential drop across the Helmholtz and Gouy layers can be neglected compared with space charge layer which is generally the case for PEC solar cells.

d] Differential capacitance and Mott-Schottky plot

Neglecting the surface states and adsorption as a first approximation, the simplest electrical equivalent of a S/E interface can be regarded as a series combination of three capacitances : C_{sc}, C_H and C_G. The total capacitance is given by

$$\frac{1}{C_T} = \frac{1}{C_{SC}} + \frac{1}{C_H} + \frac{1}{C_G} \qquad ...(4.7)$$

For moderately concentrated electrolyte, the contribution to C_T

by C_H and C_G can be ignored. Thus the total capacitance is solely that due to a space charge layer. As the surface states deteriorate the performance of a PEC cell, a model to account for the behaviour of surface states can be incorporated in the interface as shown in Fig 4.6 |63,70|. Each of the n-surface states is represented as a series combination of a capacitance (C) and a resistor (R). The surface states are in parallel with each other and the semiconductor space charge capacitance (C_{SC}). The total electrode capacitance therefore, is $C_{sc} = \Sigma Ci$. This network of parallel capacitances is in series with the bulk resistance (R_{sc}) of the material, the double layer capacitance (C_{dl}), and the solution resistance (R_{sol}) between the semiconductor and the reference electrode. Any Faradaic process will short across C_{sc} and C_{dl} as represented by Z. The analysis was simplified by controlling the conditions to minimise any Faradaic process so that Z can be replaced by an infinite impedance. Also C_{dl} is much larger than c_{sc} and can be ignored |63,70|. The measurement of a differential space charge layer capacitance provides a convenient method to analyse a S/E interface and for obtaining the useful informations about both the semiconductor and an electrolyte. For semiconductor electrolyte solar cells, the contribution to the capacitance is through capacitances due to depletion region, Helmholtz layers, and the Gouy diffused layer. Neglecting the surface states and assuming all the donors and acceptors as fully ionised, and high ionic concentration of the redox couple, the space charge layer capacitance is given by;

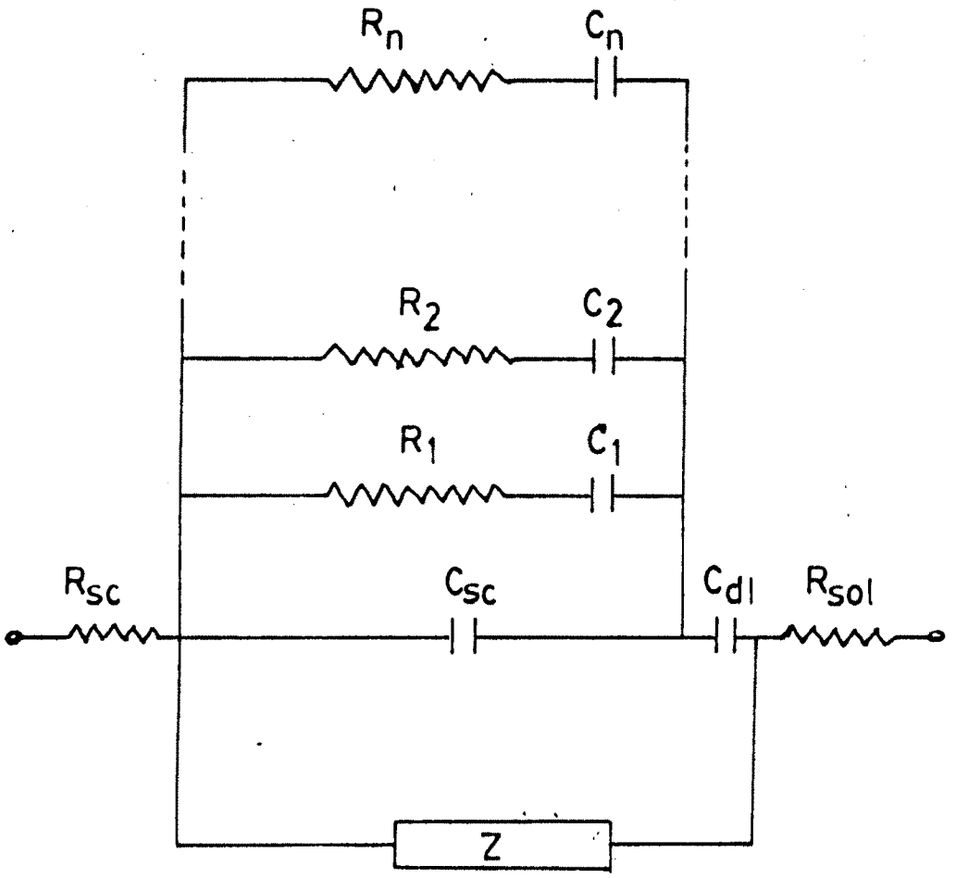

Fig-4.6 An equivalent circuit for the semiconductor/ electrolyte interface.

$$C_{sc}^{-2} = \frac{2}{\epsilon_o \epsilon_s q N_D} \left[\Phi_{sc} - \frac{KT}{q} \right] \qquad ...(4.8)$$

where, Φ_{sc} = potential in the space charge region of the semiconductor, ϵ_s = dielectric constant of the semiconductor, ϵ_o=permittivity of the free space and other symbols have their usual significance. Equation (4.8) is called as the Mott-Schottky equation, according to which C_{sc}^{-2} vs Φ_{sc} plot is a straight line. However, Φ_{sc} cannot be measured directly and is usually measured against a reference electrode (NHE or SCE). The measured potential difference, V, corresponds to :

$$V = \Phi_{sc} - \Phi_{NHE} \qquad ...(4.9)$$

where, V = electrode potential. The importance of Mott- Schottky plot is to measure the flat band potential (V_{fb}), and therefore, when Φ_{sc} = 0, the bands are almost flat. The Mott-Schottky equation under such circumstances can be written as :

$$C_{sc}^{-2} = \frac{2}{\epsilon_s \epsilon_o q N_D} \left(V - V_{fb} - \frac{KT}{q} \right) \qquad ...(4.10)$$

Therefore, a plot of C_{sc}^{-2} vs V will be a straight line and intercept with voltage axis gives the value of 'V_{fb}' and the slope gives the donor concentration. The diagrammatic representation is shown for n and p type semiconductors in Fig 4.7(a). Further, the Mott-Schottky plot determines the type of majority carriers and the band bending, V_b, which is a maximum open circuit voltage that can be obtained from a PEC cell. The V_b is related to V_{fb} as :

$$V_b = \left[\frac{E_{F,redox}}{q} - V \right] \qquad ...(4.11)$$

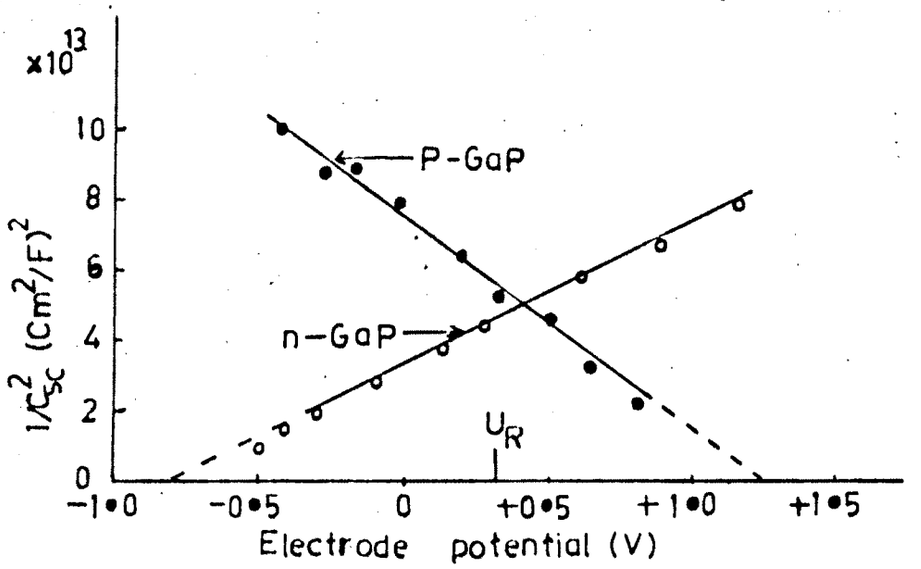

Fig-4.7(a) Mott-Schottky plots of space charge capacity for Gap electrodes vs electrode potential in 1M-H_2SO_4.

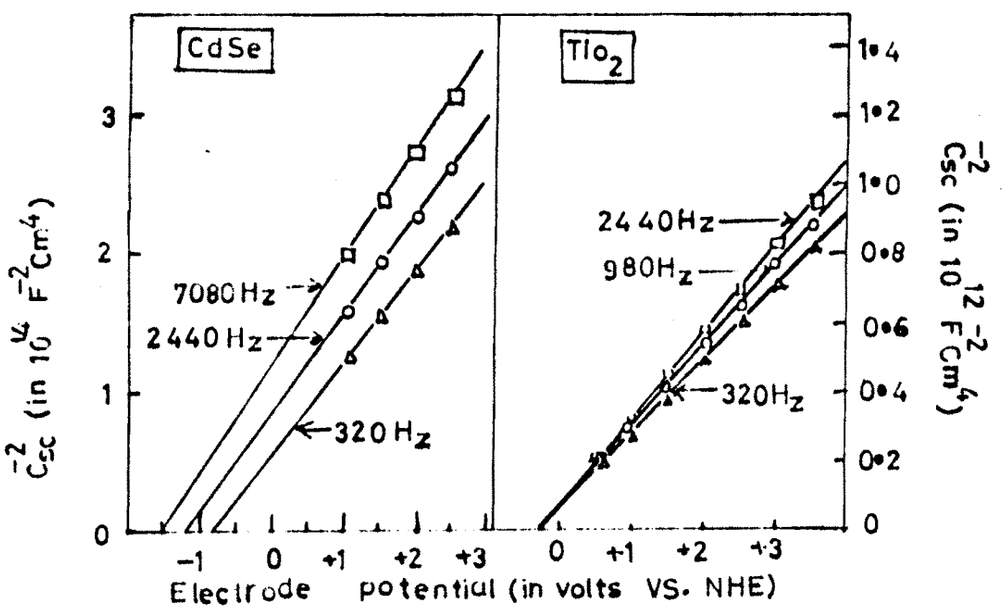

Fig-4.7(b) Mott- chottky plots for CdSe - and TiO_2 at different frequencies (electrode potential in volts vs.NHE).

where, $E_{F,redox}$ = (- 4.5 qV NHE + qV redox). Thus values of V_{redox} for many redox couples can be obtained from the data given by Latimar |71| and Lewis et al |72|. The depletion layer width and position of the band edges can be calculated using Mott-Schottky plots. In the derivation of the equation (4.10), the effects due to the electrolyte or semiconductor bulk resistance, interface as a leaky capacitance (Faradic currents), and frequency dependent dielectric constant were not taken into account and hence Mott-Schottky plots under such circumstances become frequency dependent causing frequency dispersion [Fig.4.7(b)].

The ideal Mott-Schottky behaviour is more an exception than a rule for the semiconductor electrolyte interface. The departure from an ideal behaviour has been observed for many semiconductors by various workers |73-75|. Some of the reasons for this non ideality are i] geometrical factors such as the edge effect, non-planar interface, surface roughness etc leading to non-uniform a.c. current distribution, ii] non-uniform doping, iii] presence of both donor and accepter impurities, iv] presence of deep donors and acceptors, and v] an extra contribution, `C' to the total capacitance due to : a] the presence of an oxide film, b] ionic adsorption on the surface, c] Helmholtz layer capacitance, d] existence of an acid-base equilibrium at the interface. Thus reliable data on V_{fb} and N_D can be obtained only when experiments are performed on well etched samples.

4.2.2 Mechanism of charge transfer at S/E interface

An electron may either be transferred from an electrolyte to

the electrode and vice-versa under the suitable values of valance and conduction band energies and a proper choice of an electrolyte redox couple. The ionic species will either be reduced or oxidised at the respective electrodes. In an idealised charge transfer reaction across the S/E interface, semiconductor acts only as donor or acceptor of electrons without any chemical change in its constitution.

a] Charge transfer in dark

In order to understand the charge transfer process across the electrode/electrolyte interface in dark, let us consider the motion of the ions from solution side to the electrode and back. There occurs both electronation,

$$A^+ + e^- \longrightarrow D$$

and deelectronation,

$$D \longrightarrow A^+ + e^-$$

reactions |68|.

If a positive ion moves against the field direction in an electronation reaction, it moves in the direction of field in deelectronation reaction. This is shown in Fig 4.8. Further, if the positive ions has to be activated through a potential difference `$\beta\Delta\Phi$' in electronation reaction, it has to be activated through the remainder $(1 - \beta\Delta\Phi)$ in the deelectronation reaction, where `β' is symmetry factor and Φ is a potential through which ion passes. Therefore, the rate of electronation and deelectronation reactions and respective current densities can be evaluated. The difference between deelectronation $(\overleftarrow{i})$ and electronation $(\overrightarrow{i})$ current densities gives the non-equilibrium

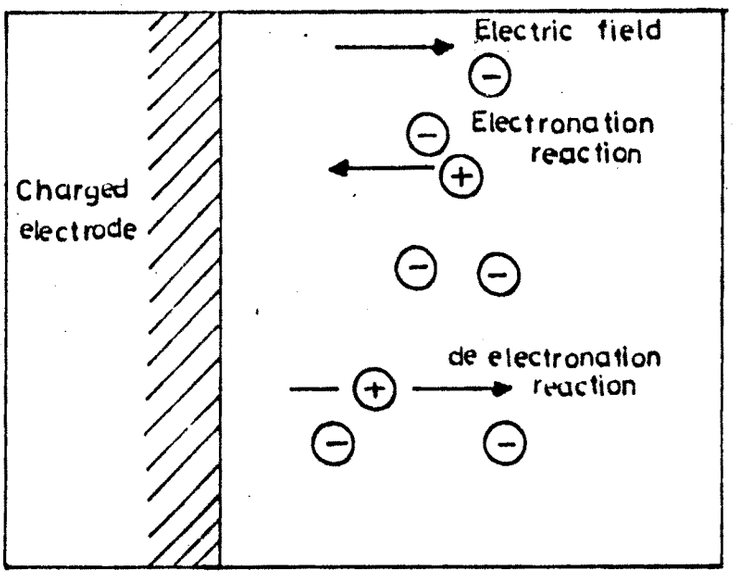

Fig-4.8(a) Electric field effect on electronation and de-electronation reactions.

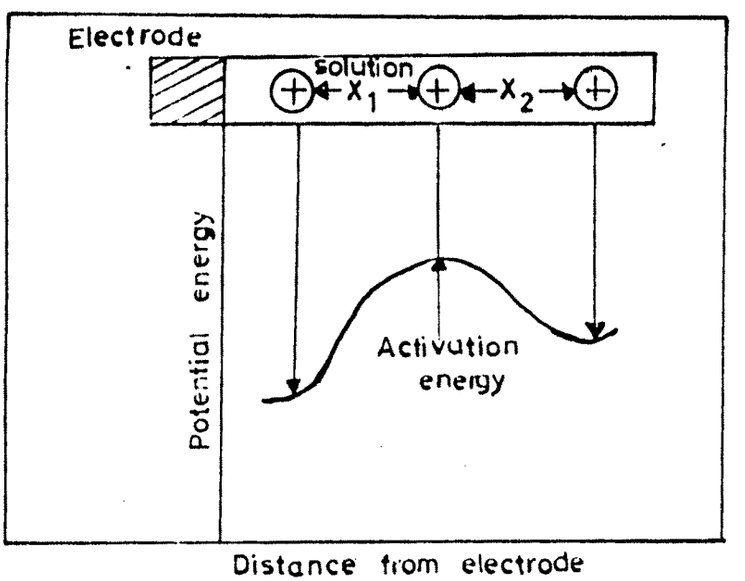

Fig-4.8(b) Construction of a potential energy distance profile by consideration of the potential energy change produced by varying X_1 and X_2.

current density (i) as :

$$i = \overleftarrow{i} - \overrightarrow{i} = F\,\overleftarrow{K_c}\,C_D \exp\left[\frac{(1-\beta)\,F\Delta\Phi}{RT}\right] - F\overrightarrow{K_c}C_A \exp\left[\frac{-\beta F\Delta\Phi}{RT}\right] \quad ...(4.12)$$

where, $\Delta\Phi$ = non equilibrium potential difference across the interface, i=corresponding current density, and other symbols have their usual significance. One can split $\Delta\Phi$ into the equilibrium ($\Delta\Phi_e$) and another portion V by which the electrode potential departs from the equilibrium,

i.e. $V = \Delta\Phi - \Delta\Phi_e$

Then we can write the net current density as :

$$i = i_o \left[\exp (1-\beta) \frac{VF}{RT} - \exp \frac{-\beta VF}{RT}\right] \quad ...(4.13)$$

Equation (4.13) is called as the famous Butler-Volmer relation |68|, and shows dependence of the current density through a metal-solution interface on the portion V. Small changes in V, produce large changes in `i'. An another important parameter is symmetry factor `ß'. In the electrode/electrolyte system, there is a hill shaped potential barrier even in the absence of an electric field as shown in Fig 4.8(b) |68|.

b] Charge transfer in light

The photogenerated carriers in the depletion region, upon illumination, are separated by an electric field at the interface |76,77|. This process results in a counter field which is maximum at open circuit condition called as `V_{oc}'. This photovoltage drags electrons from semiconductor to the counter electrode whereas, electrolyte captures the holes. The reaction as a whole can be formulated as;

i] Red (solv) + h^+ $\rightleftharpoons$ OX (solv) - At semiconductor electrode

ii] OX (solv) + e^- $\rightleftharpoons$ Red (solv)--- At counter electrode.

The electrode plays nothing in the reaction but acts only as a shuttle for charge transfer mechanism. Consider a n-type semiconductor in contact with an electrolyte under illumination and with a forward voltage V, applied. The schematic showing the energy level diagram of electron is shown in Fig 4.9. The quasi - Fermi levels for electrons (E_{Fn}) and for holes (E_{Fp}) in the depletion region are assumed flat. It is further assumed that under forward bias condition, the separation between E_{Fn} and E_{Fp} in the depletion region is `U' rather than `V' and is

$$E_{Fn} - E_{Fp} = qU \qquad ...(4.14)$$

The assumption that, U > V, represents the fact that minority carrier concentration under light is larger than its concentration in dark. For holes to flow from the semiconductor to electrolyte, U is defined from the relation;

$$\exp \frac{qU}{KT} = p\ (w)/P_o \qquad ...(4.15)$$

Where, p(w) = hole concentration at the edge of the depletion region (X=W) and P_o the hole concentration in the bulk of the semiconductor in dark at equilibrium. It is assumed that most of the applied voltage appears across the semiconductor depletion region, thus the series resistance of a cell is negligibe and an electrolyte concentration should be high enough such that C_H is atleast a magnitude greater than C_{SC}. From the depletion layer approximation, the width of the depletion layer is :

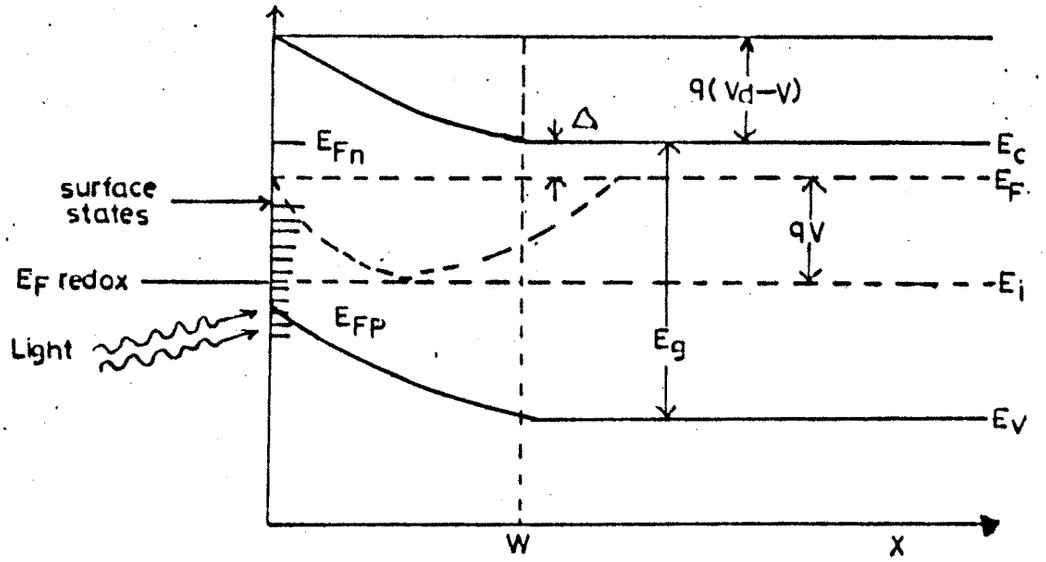

Fig.4-9 Electron energy level diagram for an n-type semiconductor photoelectrode near the S/E interface under illumination and a forward bias V reducing the band bending from qV_D to $q(V_D-V)$.

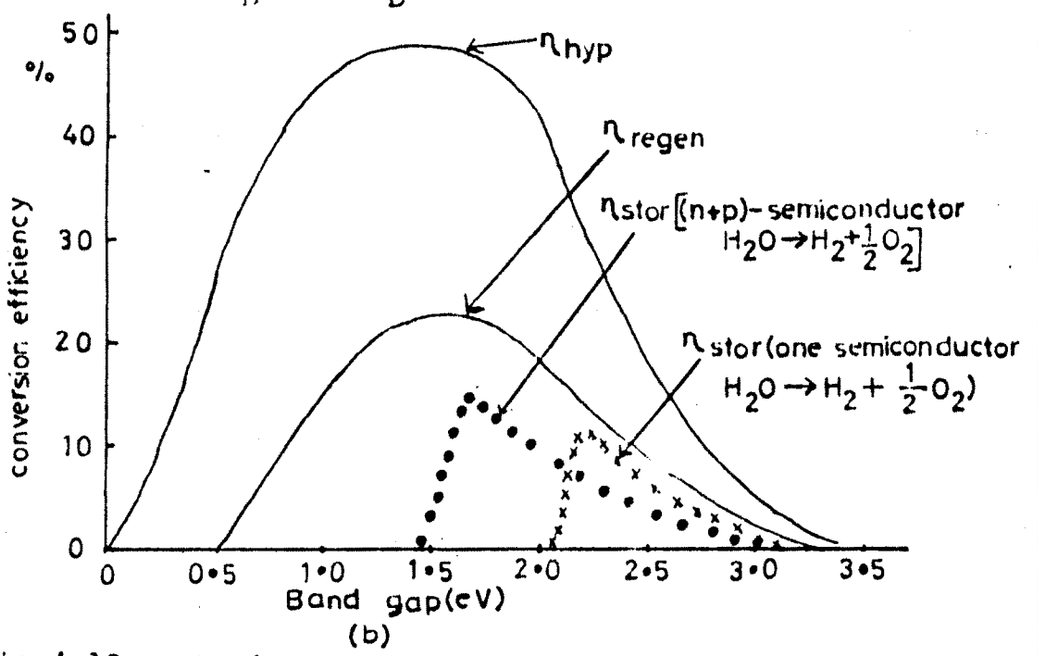

Fig-4.10 Estimated optical conversion efficiencies of the PEC solar cells for power generation (regenerative cell), η_{regen} and storage, η_{stor}. η_{hyp} is the theoretical energy conversion efficiency for AM_1 (Gerischer-1979).

$$W = W_o (V_D - V_o)^{\frac{1}{2}} \qquad ...(4.16)$$

where, $W_o = \dfrac{(2\ \epsilon_s \epsilon_o)}{qN_D}$

ϵ_s is a dielectric constant of the material and ϵ_o is the permitivity of free space, N_D is donor concentration, and V_D = equilibrium band bending voltage. If S_t is the surface transfer velocity, S_r is the surface recombination velocity, Φ_o is the incident photon flux, α is the light absorption coefficient, and W is the width of depletion region, then the photo flux can be give as

$$j_l = \left(\frac{S_t}{S_r}\right) \Phi_o \left[1-\exp\frac{(\alpha-w)}{1+\alpha t}\right] \qquad ...(4.17)$$

This is the useful photogenerated current of a solar cell |77|. The direction of this photocurrent is from the semiconductor to the electrolyte.

4.2.3 Some useful parameters

The band bending characteristic of the semiconductors at the interface limits the output voltage/power and the maximum photopotential is obtained when the bands are almost flat. The maximum photopotential is :

$$(V_{ph})_{max} = E_g/q \qquad ...(4.18)$$

The conversion efficiency of a cell (η) is defined as:

$$\eta = \frac{\text{(Output power)}}{\text{(Input power)}} \times 100\ \% \qquad ...(4.19)$$

The quantum efficiency is defined as :

$$\eta_q = \frac{\text{Number of photoelectrons flowing per unit area}}{\text{Number of incident photons with energy } h\nu \text{ per unit area}}$$

$$\eta_q = \frac{N(e)}{N(h\nu)} \qquad ...(4.20)$$

The various expressions of efficiency used by different authors are manifestation of equations (4.19) and (4.20). Neglecting the losses due to ohmic resistance, overpotential, light absorption in the solution etc, the efficiency of a photovoltaic cell amounts to |70,78|;

$$\eta = E_g \frac{\int_{E_g}^{\infty} \alpha(E)\ N(E)dE}{\int_{0}^{\infty} E.N(E)dE} \qquad ...(4.21)$$

Where, E_g=band gap of the material, N(E)=Number of photons with energy E, $\alpha(E)$=fraction of photons absorbed.

The lower limit in the integral at the numerator (Eg) is the threshold optical energy of the photons that generates e-h pairs. Equation (4.21) is suggested for the large magnitudes of band gap (Eg) and α. Further, $\alpha(E)$ near the band edge is approximated as

$$\alpha = \frac{A(h\nu - E_g)^n}{h\nu} \qquad ...(4.22)$$

where, A is constant and n=½ for direct allowed and n=2 for indirect transitions. Thus equation (4.21) contradicts equation (4.22) and `η' would be a maximum for some optimum value of E_g. The conversion efficiency has a maximum around E_g = 1.2 eV as shown in Fig.4.10. For real conversion efficiency, the following losses are to be considered |76|:

i] ohmic loss across the external load (iR_L), ii] energy lost in the separation of e-h pairs in the space charge layer, iii] losses due to minority carriers, ($q\eta_{min}$) and majority carriers ($q\eta_{maj}$) at the semiconductor and counter electrodes,

respectively. The estimated loss of energy is approximately:

$$\Delta G_{loss} \geq 0.5 + e\,(\eta_{min} + \eta_{maj}) + iR_L \qquad ...(4.23)$$

From Fig.4.10 it is clear that a theoretical efficiency of about 25% is expected for regenerative type PEC cells for a semiconductor with E_g=1.4 to 1.7 eV. The band gaps of some of the semiconductors vis-a-vis efficiency is given in Fig.4.11(a). Now it is well verse that the maximum open circuit voltage attainable from an electrochemical photovoltaic cell would be :

$$V_{oc} = V_{redox} - V_{fb} \qquad ...(4.24)$$

Thus, the ultimate efficiency would also depend upon $V_{redox} - V_{fb}$ as shown in the Fig.4.11(b).

4.3 Experimental Procedure

4.3.1 Preparation of Sb_2S_3 photoelectrode

The antimony trisulphide thin film photoelectrodes have been deposited as described in section 2.3.1 onto the mirror grade polished stainless steel substrates. The preparative conditions were selected as mentioned in the article 4.3.1. The photoelectrochemical cell was constructed using one of these samples as a photoelectrode, 0.2M Ferrocene in DMSO as an electrolyte, and CoS treated graphite rod as a counter electrode.

4.3.2 Electrical characterisation of a PEC cell

Design, fabrication, and constructional details of a PEC cell are outlined in chapter II. The charge transfer mechanism across an electrode/electrolyte interface can be understood by examining the electrical and optical properties of a PEC cell. In view to achieve this, current-voltage and capacitance-voltage characteristics have been studied. A

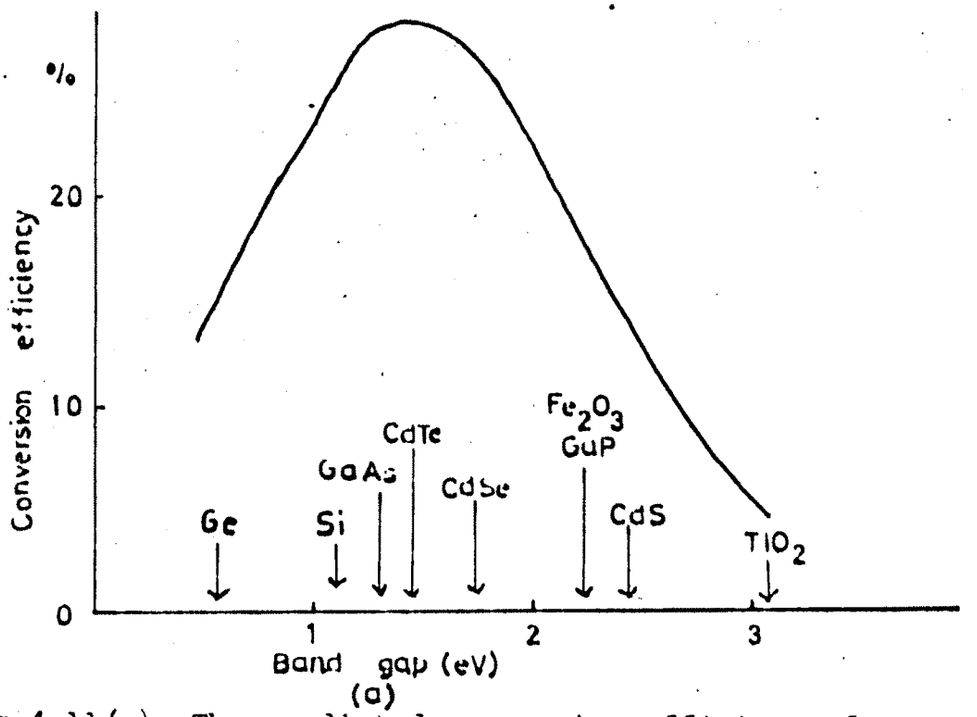

Fig-4.11(a) The predicted conversion efficiency for PEC's as a function of bandgap under AM_1.

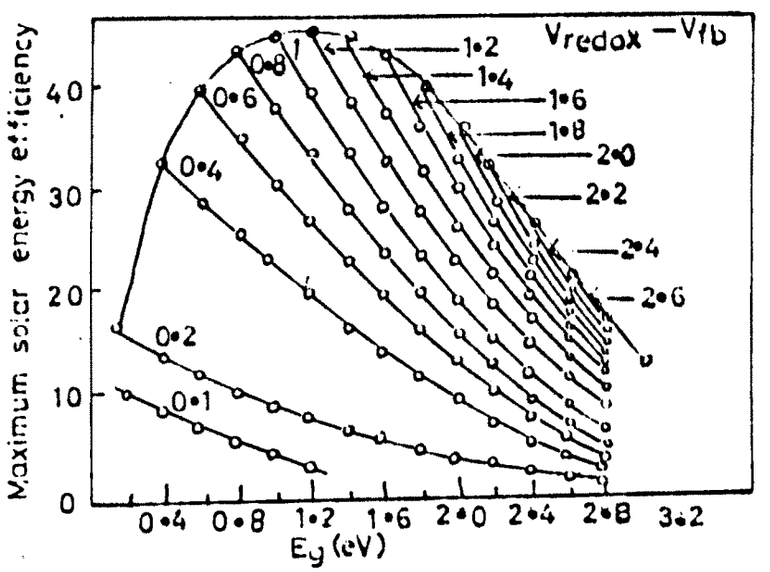

Fig-4.11(b) Maximum solar energy conversion efficiencies for open circuit solar cells with various values of Eg and $(V_{redox}-V_{fb})$, (Noufi and Warren 1980).

SHIVAJI UNIVERSITY LIBRARY KOLHAPUR

potentiometric arrangement was employed to vary the potential across the junction and current through the junction was measured with a sensitive currentmeter. The same circuit was used to measure the space charge layer capacitance. The voltage across the junction was changed in a similar fashion as that of the previous and the junction capacitance was measured with an Aplab capacitance meter. The superimposed ac voltage was 1V PP and the voltage dependent capacitance was measured at the different frequencies (i.e. 1KHz and 100 Hz). The reverse saturation current through the junction was noted between 30°C to 100°C for the calculation of barrier height. The power output characteristic was obtained under 100 mW/cm² intensity.

4.3.3 Optical characterisation of a PEC cell

The optical characterisation of a PEC cell mainly involves the measurement of photo, spectral, and speed responses.

a] Photoresponse

This involves measurement of short circuit current (I_{sc}) and open circuit voltage (V_{oc}) under various illumination intensities. The illumination was measured with a digital lux meter LX -101, and I_{sc} and V_{oc} were noted with the sensitive current and volt meters, respectively.

b] Spectral response

It was the measurement carried out, of the short circuit current for various exciting wavelengths. The wavelength range selected was 400nm to 900nm and I_{sc} was measured with a current meter, HIL-2665, 4½ digit.

BARR. BALASAHEB KHARDEKAR LIBRARY
SHIVAJI UNIVERSITY, KOLHAPUR

c] Speed of response

It is a measurement of I_{SC} or V_{OC} with time for constant illumination. Thus, V_{OC} was measured up to a steady state condition for various time intervals and then illumination intensity was made OFF and the decaying V_{OC} was also measured for different time intervals. Further cycles can be repeated.

4.4 Discussion of Results

It is now clearly understood from the several experimental evidences that when a semiconductor photoelectrode is brought in contact with an electrolyte, there occurs a drastic degradation in the performance of an electrochemical photovaltaic cell. This undesirable degradation will not allow a photoelectrochemical cell to yield the satisfactory results in a reproducible fashion. It is the photoelectrode material that governs almost all the properties of a photoelectrochemical cell which can be examined by examining the changes in its several thin film properties |37,47,70,79|. The thin film properties those contribute to the performance of a PEC cell are the electrical conductivity, carrier mobility, carrier concentration, thermoelectric properties, an activation energy, optical absorbance, mode of transition, grain dimension, nature of the material (single or polycrystal) etc. These properties and their nature of effectiveness have been described vis-a-vis in chapter III. It is now left for this chapter to observe their reflections on the cell properties. Therefore, this chapter is fully devoted for the application of thin film Sb_2S_3 photoelectrode in PEC cell. As the nature of contact between the substrate and the material

plays an important role, it has been tested. It is found that Sb_2S_3 offers an ohmic contact to the stainless steel |31|. The photoelectrochemical behavior of Sb_2S_3 (as far as scope of our investigations has been considered) has been divided into two : i) the electrical studies and ii) the optical studies.

4.4.1 The electrical studies

Electrical properties particularly, current-voltage characteristics in dark and in light, capacitance-voltage characteristic in dark, and determination of barrier height have been studied.

a] Current-voltage characteristic in dark

A PEC cell has been formed with Sb_2S_3 as an active photoelectrode. It is seen that a dark voltage, V_D, and dark current, I_D, are generated in a cell. V_D originates from the difference between two half cell potentials in a PEC cell and can be given as |80|:

$$E = E_{n\text{-}Sb_2S_3} - E_{carbon} \qquad ...(4.25)$$

where, $E_{n\text{-}Sb_2S_3}$ and Ecarbon are half cell potentials developed when electrodes are dipped in an electrolyte. It is also observed that;

$$E_{n\text{-}Sb_2S_3} < E_{carbon} \qquad ...(4.26)$$

and I_D is an indicative of some deterioration of the photoelectrode material. The dynamic I-V characteristic in dark has been studied at room temperature to understand the charge transfer mechanism across the electrode-electrolyte interface and is shown in Fig.4.12. Forward current is seen to increase rapidly with the applied voltage which can be ascribed to a small

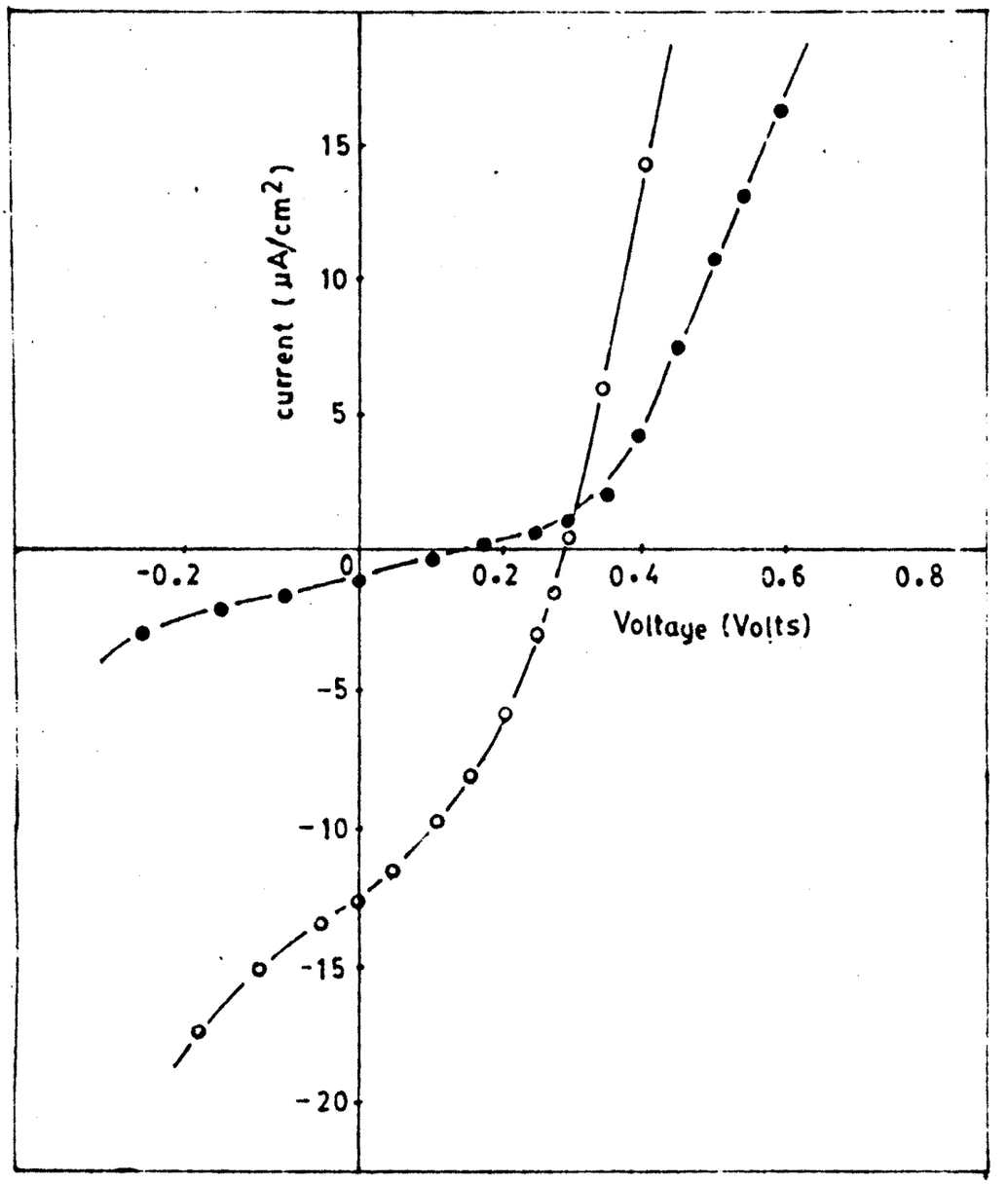

Fig. 4.12 The dynamic current voltage characteristics in; 1) ● - dark
2) o - light,
for the cell formed with n-Sb_2S_3 photoelectrode.

barrier height and increased tunneling mechanism with increase in applied bias voltage |81,82|. The nonsaturation of reverse current is due to the following reasons |80-81|: i] the effective barrier height (Φ_B) decreases because of interfacial layer, ii] electron-hole pairs, are thermally generated in the depletion layer under high applied reverse bias, and iii] the current increases due to the onset of an electron injection from the electrolyte into the semiconductor because the barrier becomes thin enough for tunneling to take place. The nature of the I-V curve can be explained by the Butler-Volmer relation as described in section (4.4.2). The magnitude of the symmetry factor `ß' is calculated from these observations and is found to be greater than 0.5 which shows that the junction formed is of rectifying type |68|. and is analogous to a Schottky barrier junction |68,80|. This is called Faradaic rectification |80|. The quality of the junction can be decided in terms of a factor, so called junction ideality factor (n_d) and therefore, the junction quality factor in dark (n_d) has been determined from the variation of log.I vs V plot. The actual determination of n_d is carried out from the high voltage linear region of the plot. The magnitude of n_d is found to be 4.62 and is relatively greater than its ideal value. The equilibrium reverse saturation current density (I_o) can be obtained from the above plot by extrapolating the straight portion of the graph to current axis. It is of the order of 10^{-7} A/cm². The higher magnitude of n_d is an indicative of non-ideal junction and this nonideality of the dark I-V characteristic can be related to the recombination mechanism and

series resistance effects |47,89|.

The built-in-potential also called as the barrier height, (Φ_B), at the junction in a cell is determined by measuring the reverse saturation current at various working temperatures in the range from 30°C to 100°C. For a Schottky barrier junction the reverse saturation current (I_o) is related to the built in potential Φ_B, as |81,83,84|:

$$I_o = AT^2 \exp(-\Phi_B/KT) \qquad ...(4.27)$$

where, A is Richardson's constant. The reverse saturation current is observed to vary exponentially with temperature. Fig (4.13) shows the variation of log (I_o/T^2) Vs 1/T and the built in potential, Φ_B, is determined from the slope of this graph. The typical value of Φ_B is 0.24 eV in our case.

b] Capacitance-voltage characteristic in dark

The electrode/electrolyte interface can further be analysed to obtain flat band potential by the measurement of space charge capacitance. It is a correlation between charge density and electrostatic potential at the interface. Since there is no any method to measure the electrostatic potential directly, the most valuable information can be obtained from the capacitance measurement of a space charge layer. Hence C-V measurement provides a convenient tool for obtaining the useful informations about both the semiconductor and an electrolyte. The flat band potential V_{fb} is an important parameter for explaining the PEC properties of the system in dark and under illumination |12,64|. It is a measure of a potential which must be applied to the semiconductor such that bands remain flat at the interface.

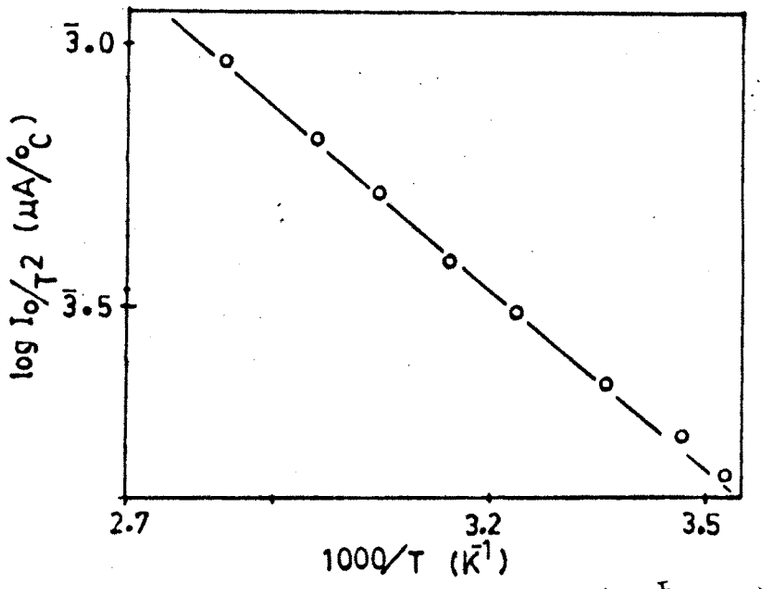

Fig-4.13 Determination of barrier height (Φ_B) of a cell from the variation of $\log(I_o/T^2)$ vs $\frac{1}{T}$)

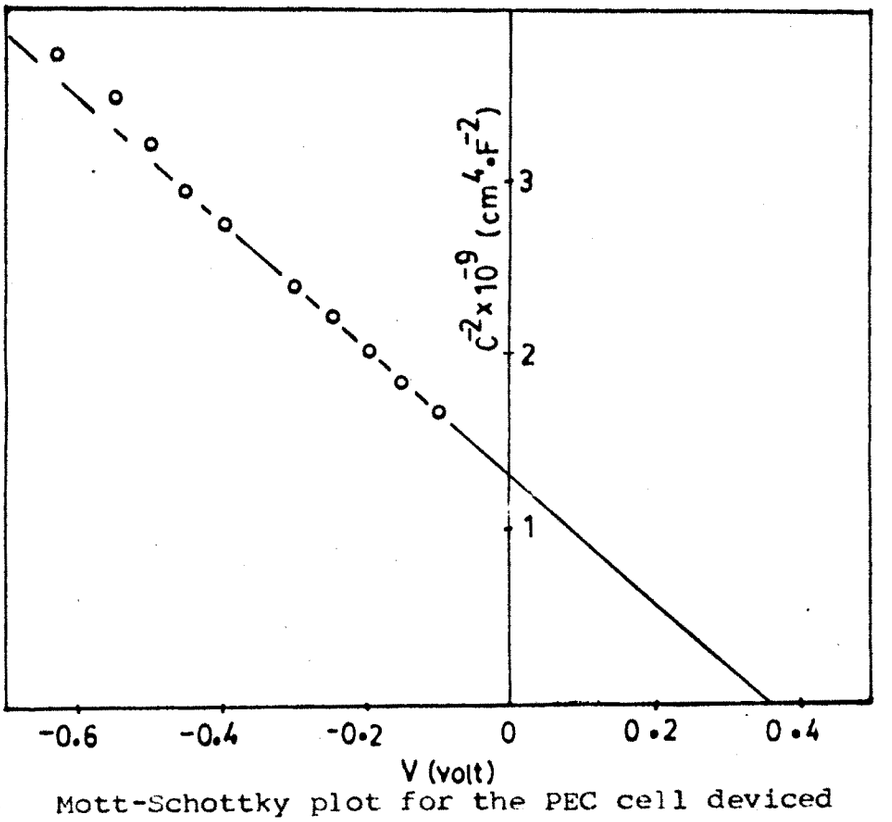

Fig-4.14 Mott-Schottky plot for the PEC cell deviced with antimony trisulphide photoelectrode.

Measurements have been made, of the junction capacitance `C' as a function of applied bias V in dark to deduce the flat band potential V_{fb}. In Fig.4.14 the plot of C^{-2} vs V is shown.

The intercept of the plot C^{-2} vs V to voltage axis gives the value of flat band potential, V_{fb}. The magnitude of V_{fb} is 0.35 V. From the Fig.4.14, it seems that the variation of C^{-2} vs V deviates from the linearity at high applied voltage levels. The non-linearity shows the graded type of junction formed |47,70| and is caused by : i] nonuniform a.c. current distribution, ii] presence of the impurities, iii] ionic adsorption on the electrode surface, and iv] presence of the surface states |47,70,85|.

C] Power output characteristic in light

The photovoltaic output curve under constant illumination intensity of 100mW/cm² was recorded and is shown in Fig.4.15. When a PEC cell is irradiated, the current-voltage characteristic shifts in a fourth qudrant, thus, indicating a generator of an electricity which is in accordance with the standard principles of the PEC cells |12,70,85,86|. It has been found that, under unbiased condition, photoelectrode becomes more and more negative upon illumination showing that the material is n-type. This is in agreement with the observations on thermoelectric power. The generation of a photovoltage and photocurrent property of a photoelectrochemical cell can be understood from the equivalent circuit of a cell. The equivalent circuit is shown in Fig.4.16. The photocurrent is represented by a current source. If the forward current in dark of a junction is I_d, then series

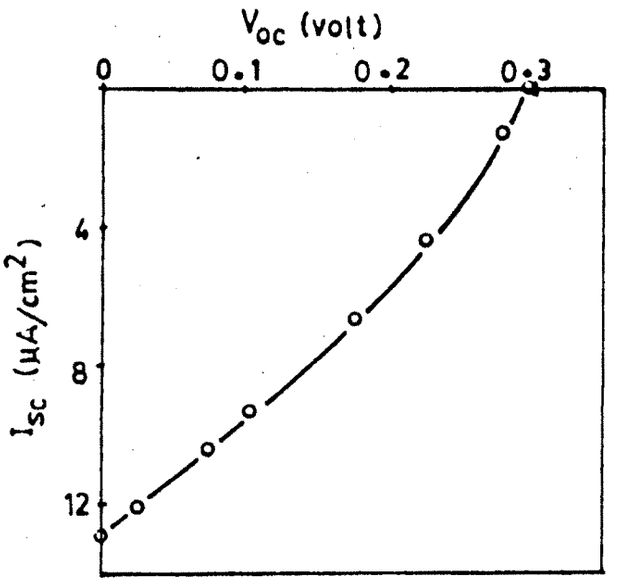

Fig-4.15 Photovoltaic power output curve under 100 mW/cm^2 intensity.

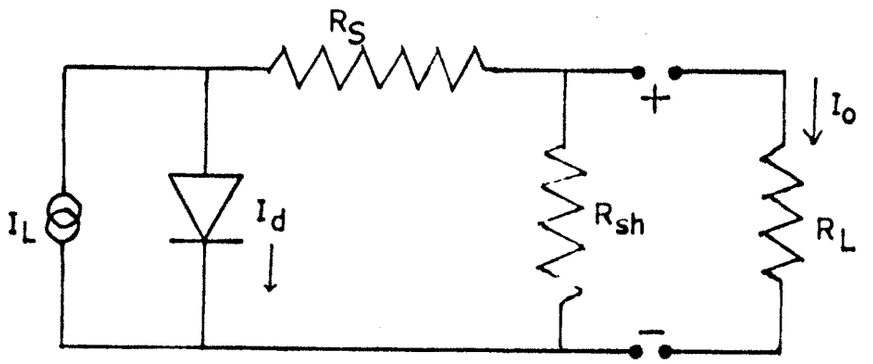

Fig-4.16 The equivalent circuit of PEC cell.

resistance of a cell can be represented by a fixed resistance `R_s' which arises mainly from the bulk resistance of a material |47,70,85,87|. The back contact of a cell is considered to be ohmic and an electrolyte offers a negligible resistance to the flow of current. The shunting paths through micropores and along the edges of the material is shown as R_{sh} |87|. R_L is the load resistance to the cell and V_{oc} is the open circuit voltage obtainable from a cell. We consider the schottky diode equation for the S/E interface and thus the total photo current of a cell under illumination can be given as |12,70| :

$$I = I_L - I_d - \frac{V_{oc}}{R_{sh}}$$

$$I = I_L - I_o \left[\exp\left(\frac{qV}{n_L KT}\right) - 1 \right] - \frac{V_{oc}}{R_{sh}} \qquad \ldots(4.28)$$

where, I_L is the photocurrent, I_d is the dark current, I_o is the reverse saturation current, and V is the applied voltage. As R_{sh} for the cell is expected to be very high V_{oc}/R_{sh} is meaningless and equation (4.28) takes the form as :

$$I = I_L - I_o \left[\exp\left(\frac{qV}{n_L KT}\right) - 1 \right] \qquad \ldots(4.29)$$

For bias voltages exceeding 3KT/q one can also neglect last term in equation (4.29). Moreover, at open circuit condition, $I_L = I_o$ and $V = V_{oc}$, thus rearrangement of equation yields |12,47,70|:

$$V_{oc} = \frac{n_L KT}{q} \ln \frac{I_{sc}}{I_o} \qquad \ldots(4.30)$$

At short circuit condition, $V_{oc}=0$, and

$$I = I_L - I_o = I_{sc} \qquad ...(4.31)$$

The I-V characteristic in light is reproduced to obtain power output at an input illumination of 100mW/cm². The series resistance (R_s) and shunt resistance (R_{sh}) have been calculated and are 14.2 KΩ and 28.67 KΩ, respectively. The fill factor (ff) of 31%, and an energy conversion efficiency (η) of 0.0012%, have been observed from these measurements.

4.4.2 Optical studies

a] Photoresponse

The photoresponse is the change in magnitudes of I_{sc} and V_{oc} with change in incident light excitation level. Thus, I_{sc} and V_{oc} were measured at different levels of incident light intensity. Variation of short circuit current I_{sc} and open circuit voltage V_{oc} as a function of light intensity is shown in Fig.4.17. It is seen that I_{sc} varies almost linearly over the whole range of light itensity under study (0 to 100 mW/cm²). However, V_{oc} saturates at high intensities which can be attributed to the presence of surface states at the electrode-electrolyte interface and unequal distribution of electrons and holes in the space charge region of the electrode |88|. The relation between V_{oc} and light intensity for equilibrium distribution of the charge carriers in the space charge region is given by equation |88|:

$$V_{oc} = \text{const.} + \frac{KT}{q} \ln F_L - \frac{KT}{q} \ln \left(V_{oc} \frac{q}{KT}\right) \qquad ...(4.32)$$

where, F_L is the light intensity and `q' is the electronic charge and all other symbols have their usual significance.

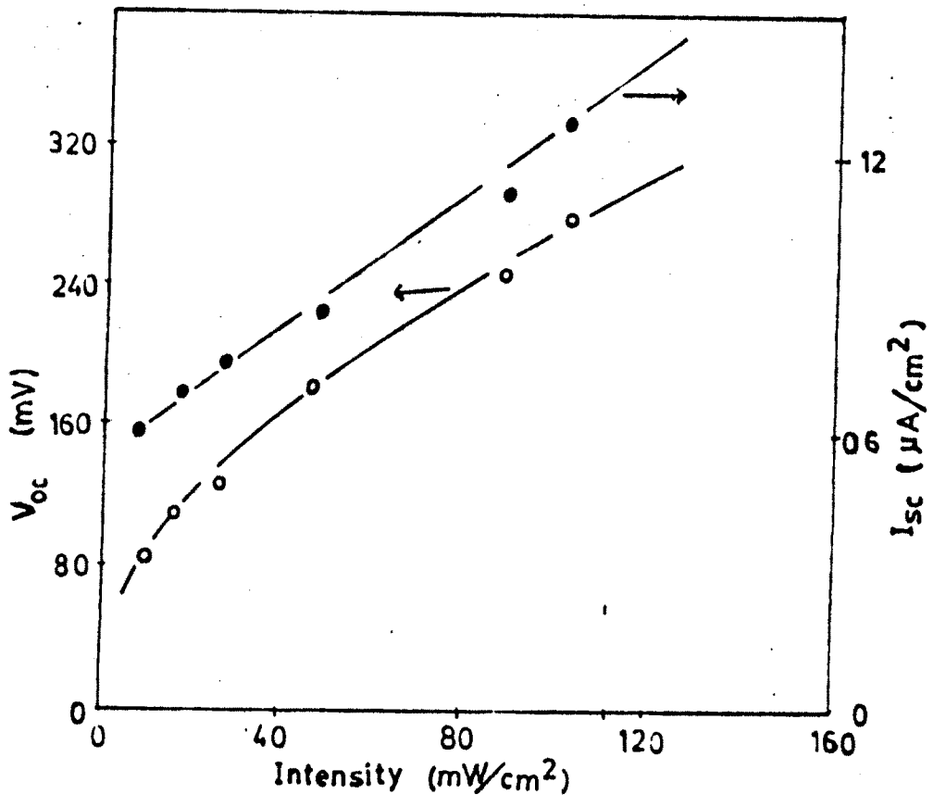

Fig-4.17 Variation of V_{oc} and I_{sc} with intensity of illumination.

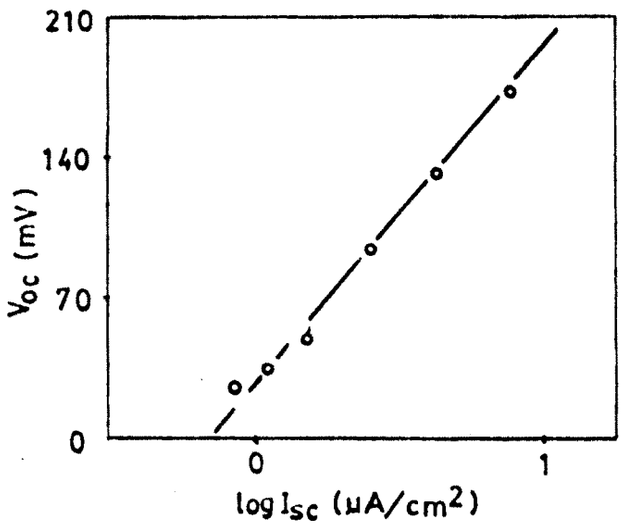

Fig-4.18 Computation of lighted ideality factor (n_L) for a cell from the variation of Voc vs. log I_{sc}.

SHIVAJI UNIVERSITY, KOLHAPUR

It is clear from the above relation that a plot of V_{oc} vs log F_L should yield a straight line. Fig 4.18 shows a plot of V_{oc} vs log F_L. The slope of this plot then permits for the estimation of junction ideality factor, n_L. The calculated value of n_L is 1.96. Alternatively, the value of n_L can be determined from the plot of V_{oc} vs ln I_{sc}.

b] Spectral response

Spectral response of a PEC cell formed with n-Sb_2S_3 thin film electrode was recorded. It is a variation of I_{sc} with the incident wavelength. Fig 4.19 illustrates the spectral response for the cell. A study of the spectral response of a PEC cell is important since, it is directly related to the solar specturm. It gives informations which are useful in identifying the recombination centres and consequently in diagnosing the problems those lead to the efficiency losses. Generally, decrease in photocurrent on shorter wavelength side of the peak is attributed to the : i] light absorption in the electrolyte, ii] surface recombination of the minority carriers, presumably mediated by the electronic states in the band gap region |88,89|. The decrease in photocurrent on longer wavelength side is because of the nonoptimised thickness and transition between the defect levels |89|. Moreover, the photons near the band edge penetrate deep into the semiconductor bulk thus the photogenerated minority carriers (holes in our case) have longer path to traverse to reach the interface and oxidize the reducing ions of the electrolyte solution. In the present study spectral response of a PEC cell is not corrected for the reflection and absorption

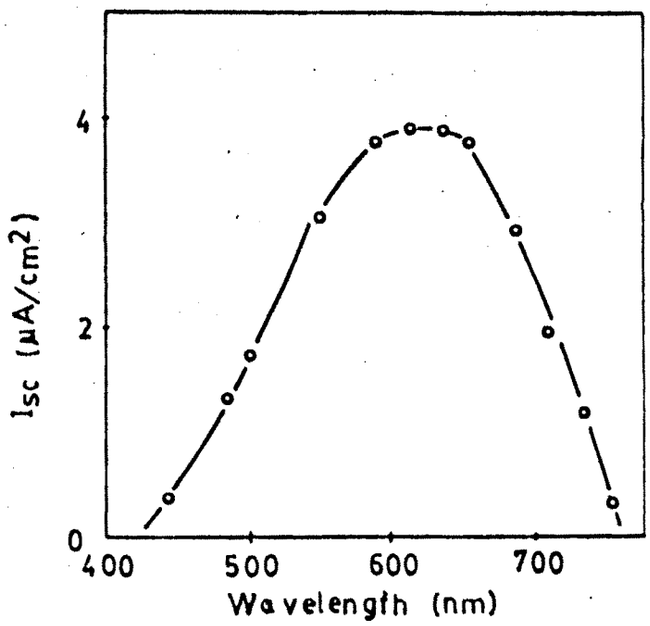

Fig-4.19 Spectral response of a cell.

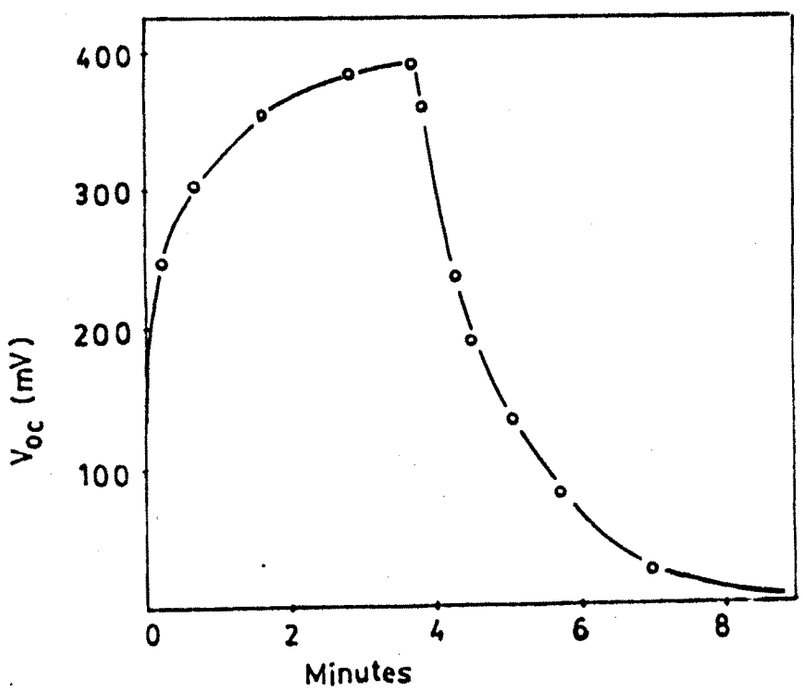

Fig-4.20 Speed of response of a PEC cell showing variation of V_{oc} with time.

losses.

c] Speed of response

Study of the I_{SC} and V_{OC} decay with time is important to know the charge transfer mechanism of the semiconductor/electrolyte junctions. Fig 4.20 shows V_{OC} decay with time for a cell under 100 mW/cm² light excitation. Relatively fast rise and slow decay is observed in the present study which is attributed to the adsorption of electrolyte melecules on the surface of the photoelectrode under light excitation |89| and dense population of the surface states at the interface. It is not possible to find out the minority carrier life time by the V_{OC} decay technique, as most of the role of charge transport is played by the ions in an electrolyte.

4.5 <u>Conclusions</u>

A photoelectrochemical cell formed with n-Sb_2S_3 photoelectrode has an efficiency lower than that of the expected. It shows poor performance relative to the cell formed with other materials. The major reason is its high electrical resistivity. In order to improve the performance of Sb_2S_3 based PEC cells, it is essential to reduce its resistivity drastically by optimising various parameters and deposition conditions such as : Sb:S ion ratio, thickness, dopant concentration, post preparative treatments, selection of a proper electrolyte etc. The attempts in this direction are now in progress.